Polydispersity Effects in the Evaporation of Perfluoropolyether Thin Films

Michael Stirniman* and Jing Gui

Seagate Recording Media, 47010 Kato Road, Fremont, California 94538

Received: January 16, 2002; In Final Form: April 10, 2002

The evaporation rates of bulk liquid and thin films of an alcohol-derivatized perfluoropolyether have been studied experimentally and computationally. We find that, even in the case of narrowly fractionated material, the time dependence of the evaporation rate in both the bulk and thin-film cases is dominated by the residual polydispersity of the samples. The bulk and thin-film evaporation can be described very well by a model that incorporates the molecular weight distribution, molecular-weight-dependent Arrhenius parameters of evaporation, and Raoult's law of vapor pressures. Minor corrections to the model that account for surface interactions are necessary in the case of thin film evaporation.

Introduction

Virtually all thin film magnetic media produced today for use in the disk-drive industry are supplied with a protective overcoat system consisting of hard carbon on the order of 5 nm thick, and a topical coating of some type of perfluoropolyether (PFPE) lubricant on the order of 1−2 nm thick.[1] At this thickness, the coverage of the lubricant on the carbon overcoat is only 1 to 2 monolayers (ML). These 1−2 ML of lubricant, in combination with the 10−15 ML of carbon in the overcoat, are the only protection provided the surface of the relatively soft magnetic alloy recording medium from physical damage caused by contact with the read−write head. For example, in a contact−start−stop (CSS) type of disk drive the flying read−write head lands and slides on the disk whenever the drive is powered down, and slides and takes off from the disk when the drive is restarted. In CSS reliability testing, these ultrathin carbon/lubricant overcoat systems have been routinely shown to prevent physical damage to the magnetic alloy through 20 000 start−stop cycles. In addition to providing wear resistance, the overcoat system serves a second function, namely, protecting the magnetic alloy from oxidative corrosion. Again, in component-level reliability testing the overcoat system has been shown to prevent corrosion of the magnetic layers even under relatively extreme environmental conditions, e.g., 80 °C and 80% relative humidity over several days. Because of their importance in the data storage industry, and because they are in such widespread use, the physical and chemical properties of these PFPEs are of great interest to researchers working in the area of disk-drive tribology. Among the many properties of these materials that have been studied to-date are the effects of ultraviolet and low-energy electron irradiation,[2,3] their catalytic stability in the presence of Lewis acids,[4−6] their intrinsic thin-film diffusion rates on silicon and carbon,[7−14] and the thin film diffusion response to shear forces at the top layer.[15]

All of these studies are complicated to some degree by the fact that the PFPE lubricants supplied to the disk-drive industry are not pure materials, but are rather a mixture of many different molecular weight components. While chemically similar, the components can have very different physical properties, e.g., viscosity and volatility. In many of the previous experimental studies the as-supplied PFPE materials were further fractionated, usually by supercritical fluid extraction (SFE) in CO_2, to yield samples with much narrower molecular weight distributions. The molecular weight distribution of a polymer can be characterized to some extent by the polydispersity index (PDI), defined as the mass average molecular weight M_w divided by the number average molecular weight M_n, which are given by

$$M_n = \frac{\sum_i n_i M_i}{\sum_i n_i} \tag{1}$$

and

$$M_w = \frac{\sum_i n_i M_i^2}{\sum_i n_i M_i} \tag{2}$$

where n_i is the number of molecules of component i and M_i is the molecular weight of component i. The PDI of perfluoropolyethers as supplied by the manufacturer is typically in the range of 1.2 to 1.5.

In previous papers, we reported on the bulk evaporative properties of PFPEs as measured by thermogravimetric analysis (TGA).[16,17] In ref 17, we showed that the polydispersity has a large effect on the evaporation rate of a bulk liquid sample of an alcohol-derivatized PFPE, Fomblin Zdol, even when such a sample has been fractionated to the point that its molecular weight distribution would be considered very narrow by disk-drive tribology standards (i.e., PDI ∼1.05). The effect of the polydispersity on the evaporation rate is solely the result of the molecular weight dependence of the volatility for the different components of the mixture, and can be quantitatively modeled by assuming that the liquid lubricant is an ideal solution.

In this paper we extend those bulk evaporation experiments to thin films of PFPE on the surface of carbon-coated magnetic media. In recent similar experiments, Tyndall and Waltman reported on observations of nonclassical first-order desorption

* Author to whom correspondence should be addressed. E-mail: Stirniman@seagate.com.

10.1021/jp020128y CCC: $22.00
Published on Web 05/17/2002

kinetics of PFPE films in the monolayer regime. They proposed that the desorption kinetics be fit with time-dependent rate constants, which were attributed to thickness-dependent surface free energy changes.[18] We have observed identical behavior in our experiments, and while the films used in the present work, at $\sim 4-15$ ML, are somewhat thicker than the films used in that reference, we believe that our results clearly show that the dominant factor contributing to the nonclassical evaporation kinetics of these films is their polydispersity.

Experimental Section

The TGA experiments on the bulk liquid evaporation were carried out in a Rheometrics model STA-625, which has a temperature range from liquid nitrogen temperatures to 625 °C, and was operated at a mass resolution of 0.3 μg. Typical sample sizes were on the order of 25 mg. Evaporation rate data were collected by ramping the temperature linearly at 10 °C/min to a selected isothermal temperature, under a dry nitrogen purge. The nitrogen purge rate was typically 20 mL/min. However, in earlier experiments the evaporation rates were shown to be insensitive to this parameter as it was varied between 10 and 80 mL/min. Samples were contained in cylindrical aluminum pans, 2 mm high by about 5.5 mm diameter.

Relatively monodisperse Zdol was prepared by SFE of Zdol 4000, to produce nine fractions with M_n ranging from 1040 to 6710 amu. A tenth fraction comprised the residuals from the extraction process and was not used in these experiments. The M_n of each fraction was determined using ^{19}F nuclear magnetic resonance (NMR) spectroscopy. Further fractionation of the lowest molecular weight Zdol fraction from SFE was accomplished by vacuum distillation at about 10^{-4} mbar in a Kugelrohr apparatus. The PDI and molecular weight distribution of each SFE fraction were determined by size exclusion chromatography (SEC) using a Hewlett-Packard model 1050 HPLC with a Polymer Laboratories column and evaporative mass detector, with 1,2-dihydroperfluoropentane (Vertrel-XF, DuPont) as the solvent. The SEC column was calibrated iteratively using the nine SFE fractions, by adjusting the molecular weight associated with the peak retention times until the known number average molecular weights were returned from the molecular weight distributions. The PDIs of the SFE fractions were typically on the order of 1.05 to 1.10. The M_n and PDI of the Zdol fraction used in this work were 1040 amu and 1.05, respectively.

The Zdol thin films were deposited on carbon-coated magnetic media using a dip-coating method,[17] again with Vertrel XF as the solvent. The thicknesses of the thin films were measured by monitoring the intensity of the broad peak associated with the C−F stretching and bending vibrations using Fourier transform infrared spectroscopy (FTIR), which was calibrated against thickness standards measured with X-ray photoelectron spectroscopy (XPS).

Simulated TGA curves were obtained using the LSODE package (Livermore Solver for Ordinary Differential Equations[19]).

Results and Discussion

A. Bulk Liquid Isothermal Evaporation. The model used to describe the evaporation of a bulk ideal PFPE is described in ref 17. Briefly, the experimentally measured evaporation rate of a polydisperse liquid of constant surface area will be given by

$$\frac{dW}{dt} = \sum_i \frac{dm_i}{dt} \cdot M_i = \sum_i \chi_i(t)\, \nu(M_i) \exp\left(-\frac{E_a(M_i)}{k_b T}\right) \quad (3)$$

where i refers to the individual molecular weight components, dW/dt is the total mass evaporation rate, dm_i/dt is the component molar evaporation rate, M_i is the molecular weight of each component, $\nu(M)$ is the Arrhenius preexponential factor, $E_a(M)$ is the activation energy for evaporation, k_b is Boltzmann's constant, and T is the temperature. The mole fraction of each component in the liquid phase is given by

$$\chi_i(t) = \frac{m_i(t)}{\sum_i m_i(t)} \quad (4)$$

where the time dependence of the mole fractions is written explicitly to emphasize that the liquid phase molecular weight distribution evolves as lighter molecular weight components are preferentially evaporated.

If the initial mole fractions at $t = 0$ and the molecular weight dependencies of the Arrhenius parameters are known, eq 3 can be solved numerically to predict the evaporation rate of an ideal bulk polydisperse liquid. This method was used in ref 17 to accurately predict the bulk evaporation rate of a low molecular weight polydisperse Zdol sample during temperature ramp TGA, using initial mole fractions given by the SEC molecular weight distribution, and Arrhenius parameters measured in separate TGA experiments.

The initial molecular weight distribution of the low molecular weight Zdol fraction used in these experiments is shown in histogram form in Figure 1, and the empirically determined molecular weight dependencies of the Arrhenius parameters over the range 450 to 2400 amu obtained in ref 17 are given by

$$\nu = 5.3 \times 10^7 \exp(0.0017M) \text{ mg/s} \quad (5)$$

$$E_a = 59.1 + 0.031M \text{ kJ/mol} \quad (6)$$

The activation energy, i.e., heat of vaporization, for 1300 amu Zdol predicted by eq 6 is about 99 kJ/mol. This is in close agreement with the activation energy for desorption of multilayers measured in very recent temperature-programmed desorption experiments by Paserba and Gellman for an essentially monodispersed Zdol at the same molecular weight, 97 ± 1 kJ/mol.[20]

Figure 2 and Figure 3 show, as a function of time, the experimentally determined weight and the evaporation rate, respectively, of the 1040 amu Zdol sample at two isothermal temperatures, 130 °C and 140 °C. For these experiments, the temperature was ramped linearly to the isothermal temperature, then was held constant to within 0.5 °C for the remainder of the TGA run. If such a bulk sample were a *pure* monodisperse liquid, constrained by a cylindrical pan to constant surface area, at a constant temperature the mass would be expected to decrease linearly, and the evaporation rate would be expected to remain constant. As the data show, the evaporation rates at both of the isothermal temperatures are quite time dependent, a result that can only be attributed to the polydispersity of the sample.

To further illustrate this point, Figure 4 shows the experimentally measured isothermal evaporation rate for a pure liquid; distilled water. After the instrument has stabilized at the isothermal temperature of 50 °C, the evaporation rate remains

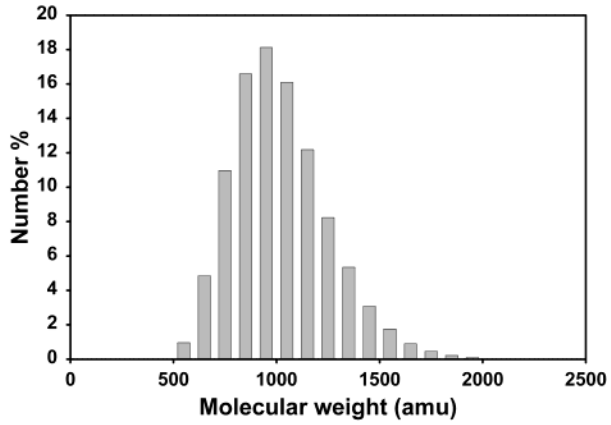

Figure 1. Histogram approximation of the molecular weight number distribution of the low molecular weight Zdol fraction as measured by SEC.

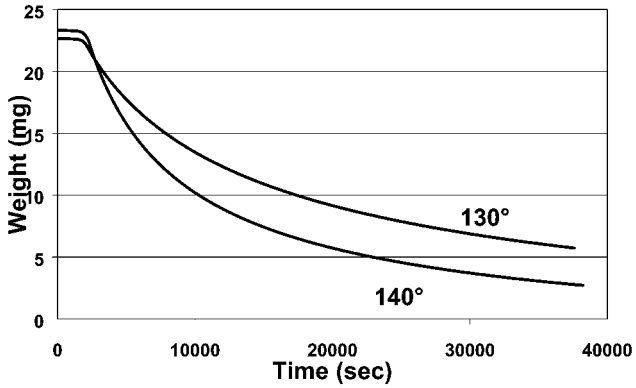

Figure 2. Experimentally determined weight as a function of time for a bulk liquid sample of the low molecular weight Zdol, at two isothermal temperatures. If the sample were a pure (monodisperse) liquid, the weight would be expected to decrease linearly over time.

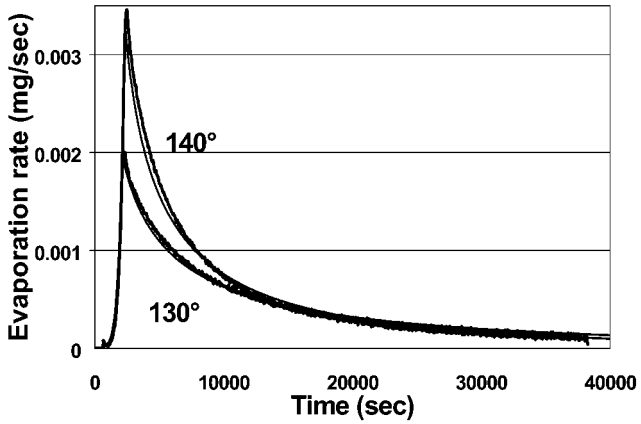

Figure 3. Experimentally measured evaporation rate as a function of time for a bulk liquid sample of the low molecular weight Zdol, at two isothermal temperatures. The smooth solid lines slightly under the data curves are the simulated evaporation rates predicted by eq 3. After the initial rise due to the temperature ramp, at the isothermal temperature the evaporation rates deviate substantially from the constant rates expected for a pure liquid, a result entirely due to the polydispersity of the sample.

essentially constant for a time corresponding to the loss of approximately 70% of the original mass of the sample.

B. Thin Film Isothermal Evaporation. The extension of the model used to describe the evaporation of a bulk polydisperse liquid to the evaporation of a nanometer scale thin film requires a number of assumptions. First, because we use infrared spectroscopy to measure the film thickness, it must be assumed that the mass evaporation rates measured for the bulk liquids can be converted to nanometer scale thickness changes; i.e., that the density of the thin film is identical to the density of the bulk liquid. In addition, as a corollary it must be assumed that the FTIR technique measures an actual physical thickness. XPS, the method used to calibrate the FTIR, itself requires a number of parameters, e.g., the carbon photoelectron escape depth through the PFPE film. As is well-known in the disk-drive industry, different manufacturers use different parameters in their calibration of lubricant thickness standards, resulting in film thickness discrepancies of up to 40%. Finally, the model of bulk liquid evaporation does not include terms for the interaction of the lubricant with the surface, which in our experiments was a carbon overcoat doped with both hydrogen and nitrogen. While it is true that at some point as the lubricant thickness increases the surface interactions can be neglected, this is unlikely to be the case at thicknesses in the 3−5 ML regime, and it is almost certainly not the case when discussing the desorption of the monolayer of lubricant adsorbed directly on the carbon surface. The last monolayer of lubricant will in general have substantially higher activation energy for desorption than the multilayers above it. Furthermore, the kinetics of desorption of the monolayer should be first order in the amount of lubricant, as opposed to the zero-order kinetics of the multilayers used in the model.

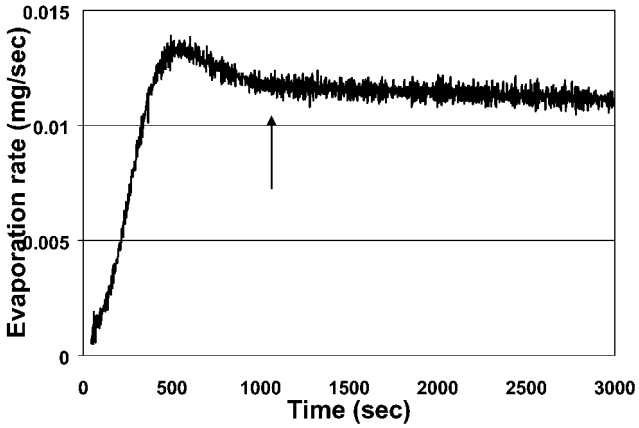

Figure 4. The evaporation rate of distilled water at 50 °C. The arrow denotes the time at which the instrument had stabilized at the isothermal temperature. In contrast to Figure 3, the evaporation rate for this pure liquid is essentially constant over the first 3000 s, accounting for about 70% of the initial mass of the sample.

Even though long-range attractive van der Waals interactions and short-range physi- and chemisorption interactions are expected to slow the evaporation rate of a thin film as compared to the bulk liquid, their effects on the measured evaporation rate must be considered in parallel with the effect of the polydispersity. As Figures 3 and 4 show, even in the total absence of surface interactions, the evaporation rate of a relatively monodisperse lubricant is markedly affected by the polydispersity. Thus it is reasonable to expect that the polydispersity could also dominate the kinetics of thin film evaporation, especially in the case of multilayer films.

Figure 5 shows the thickness vs time for an initially 145 Å thick film of the low molecular weight Zdol evaporating from a carbon-coated magnetic disk at room temperature, over a period of about 12 days. At this initial thickness surface interactions are minimal, and again the effect of the polydispersity is clearly seen in the nonlinear decrease in film thickness over time. In fact, the general shape of this curve closely resembles the shape of the weight vs time curve for the bulk

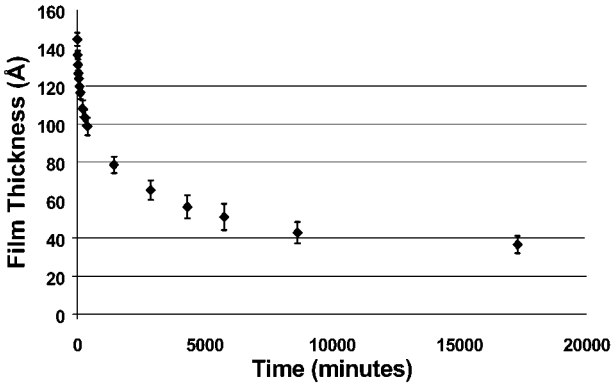

Figure 5. Film thickness vs time for an initially 145 Å thick film of low molecular weight Zdol, allowed to evaporate from a carbon-coated magnetic disk at room temperature. Similar to Figure 2, the nonlinear decrease in film thickness is almost entirely due to the polydispersity of the lubricant.

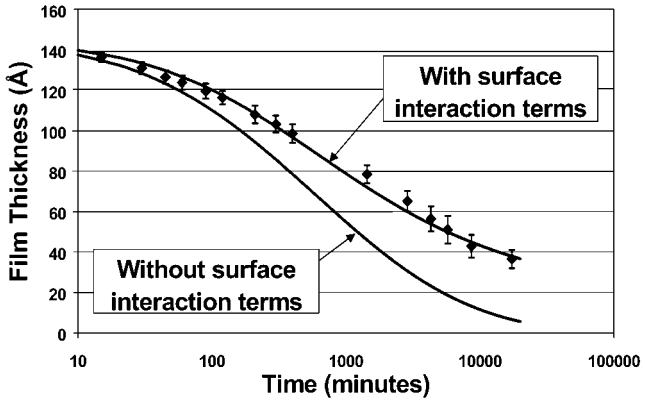

Figure 6. The data of Figure 5 on a logarithmic time scale, with model fits as explained in the text. It was found that additional surface interaction terms that varied as $1/h^3$, $1/h^2$, and $1/h$ were necessary for reasonable agreement of the model with the experimental data.

liquid in Figure 2, where the nonlinear decrease was entirely due to the polydispersity of the sample. Similar thickness vs time curves were obtained in thin film evaporation experiments using three other initial thicknesses: 42 Å, 77 Å, and 101 Å.

C. Surface Interaction Effects. Figure 6 shows the data of Figure 5 with the time axis converted to a logarithmic scale. The solid lines in Figure 6 are the results of the model calculation for this system, obtained by converting the bulk mass evaporation rates of eq 3 to thickness changes, using the Zdol bulk density of 1.8 g/cm^3. If surface interactions are neglected (lower solid curve), the general shape of the thickness vs time curve is reproduced quite well by the model, especially during the initial rapid decrease in thickness over the first hour. However, as the film thickness decreases the discrepancy of the model with the experimental data becomes more pronounced, indicating the possibility of surface interaction effects.

Incorporation of surface effects into our model covered several iterations. A first attempt to include lubricant−surface interactions was made by modifying the model to include the effects of dispersive interactions only:

$$\text{Rate} = \sum_i \text{Rate}_{0i} \exp\left(-\frac{\Pi V_i}{RT}\right) \tag{7}$$

where Rate_{0i} are the terms inside the sum in eq 3, V_i is the molecular volume of component i (derived from the bulk density and molecular weight), R is the universal gas constant, and T is the absolute temperature. Π is termed the disjoining pressure, and is given by

$$\Pi = \frac{A}{6\pi h^3} \tag{8}$$

where A is known as the Hamaker constant, and h is the film thickness.[21] For two reasons, it was found that dispersive-only interactions were insufficient to explain discrepancies of the model with the experimental data. First, the Hamaker constant required for a reasonable fit to the data for the initially 145 Å thick film was about 5×10^{-17} J, which is about 2 orders of magnitude larger than is typical for van der Waals interactions. Second, a single value of the Hamaker constant was inadequate for a reasonably good fit to the data for all four initial thicknesses of Zdol.

The fact that dispersive interactions alone are insufficient to explain the decrease in evaporation rate with decreasing film thickness over that predicted by the polydispersity alone is not surprising. Zdol, with the chemical structure $HOCF_2CF_2-(OCF_2CF_2)_m(OCF_2)_nO-CF_2CH_2OH$, can have significant polar interactions with a carbon surface through its hydroxyl endgroups. This is especially true for the relatively low molecular weight molecules considered here. In addition, there is the possibility of even stronger hydrogen bonding interactions of the alcohol endgroups with functionalized carbon groups at the surface, and with its strongly electron withdrawing CF_2 groups adjacent to the CH_2OH group of the alcohol, Zdol may even deprotonate under some conditions, leading to very strong ionic interactions. As the film thicknesses approach the molecular dimensions of the perfluoropolyether, there is also the possibility that conformational effects will introduce thickness-dependent interactions. For example, spreading studies have shown that these functionalized perfluoropolyethers form relatively complicated layered structures on a carbon surface.[11−14] Finally, there is the additional possibility of a thickness dependence of the molecular weight distribution itself, with for example the shorter, more polar molecules segregated near the PFPE/carbon interface. We have attempted to account for these additional interactions by adding two more terms to (7), similar in form to the term for the effect of the disjoining pressure, but varying in the film thickness as $1/h^2$ and as $1/h$. The results of the model after incorporating surface interaction terms over all three of these length scales is the upper solid curve of Figure 6. We would like to stress that this model is purely empirical, and that at this point we have no physical explanation for the two additional interaction terms. While it seems intuitive that dispersive terms alone should not be able to capture the complicated nature of the Zdol-surface interaction, the excellent fit shown in Figure 6 may be entirely due to the arbitrary addition of more parameters to the model. On the other hand, we would like to note that the addition of both the $1/h^2$ and the $1/h$ terms was necessary to bring the Hamaker constant for the dispersive interactions into the physically reasonable range of 3×10^{-19} J (the two additional terms in the disjoining pressure became B/h^2 and C/h, with $B = 8 \times 10^{-12}$ N, and $C = 2 \times 10^{-2}$ N/m). In addition, the use of all three surface interaction terms was necessary to fit the data at all four initial thicknesses with the same set of parameters, and all three of the parameters were needed to fit the data at any given initial thickness.

As an example, Figure 7 shows the model developed from the data in Figure 6 applied to the experimental data obtained from an initially 42 Å thick film of the low molecular weight Zdol. Despite the much lower initial thickness, the experimental thickness vs time curve shows the same general shape as that

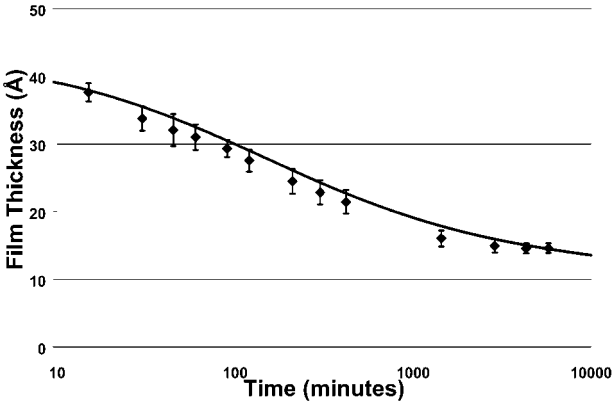

Figure 7. Application of the polydisperse evaporation model to an initially 42 Å thin film of Zdol. Despite the lower initial thickness, the overall shape of this curve is very similar to those of Figures 5 and 6.

obtained from both the bulk isothermal and the 145 Å thin film. Due to the smaller absolute amounts of the more volatile lower molecular weight components in this thinner film, the rapid initial drop in thickness occurs faster than in the thicker 145 Å initial thickness. An interesting comparison can be made between the data in Figure 6 and Figure 7, as a final illustration of the effect of the polydispersity on the evaporation rate. Over the first 1000 min, the initially 42 Å film loses more than one-half of its thickness, while the initially 142 Å thick film, after it has reached 42 Å, loses at most a few angstroms more in the same period of time. If the PFPE films were of constant composition during the evaporation, the method of preparing an initially 42 Å thick film would not affect the subsequent evaporation kinetics. However, the 42 Å film prepared by evaporation of the initially 142 Å film is of substantially higher average molecular weight than the 42 Å film prepared from the original molecular weight distribution, and consequently has a much lower overall evaporation rate.

Conclusions

Perfluoropolyether lubricants, even after extensive fractionation, are polydisperse mixtures containing a range of molecular weight components. If a component's volatility is a strong function of its molecular weight, then the effects of the polydispersity can be expected to have a correspondingly strong effect on the evaporation rate of the mixture. Using thermogravimetric analysis to measure the bulk evaporation rate of polydisperse samples of Zdol PFPE, we have shown that this is indeed the case. A model that assumes that the Zdol solution is ideal, in the sense that it obeys Raoult's law of vapor pressures, quantitatively predicts the evaporation rate of the mixture from the component evaporation rates and the initial molecular weight distribution. The model accurately predicts evaporation rates during temperature ramp TGA experiments, as well as during isothermal TGA experiments at various temperatures.

For the isothermal bulk evaporation of Figure 3, the large deviation of the evaporation rate from the expected zero-order kinetics can only be attributed to the polydispersity, and in the case of evaporation of multilayer thin films of Zdol from a carbon-coated magnetic disk, the overall deviations of the evaporation kinetics from zero-order were very similar to those seen with the bulk liquid. The similarities strongly suggest that the nonclassical thin film evaporation kinetics of Zdol are dominated by the polydisperse nature of the PFPE. In fact, the same model that was used to fit the bulk evaporation data, scaled by the PFPE bulk density, can be used to predict the thin film evaporation rate to a large extent. After terms incorporating thickness-dependent surface interactions over three length scales were added to the model, the prediction of the experimental data became quantitative. There are a number of sources of possible error in our treatment of surface interactions in the model: in particular, the continued assumption of zero-order kinetics as the film thickness approaches a monolayer, and the assumption that the thin film evaporation rates can be extrapolated from bulk rates using the bulk density. However, while the model of surface effects is admittedly incomplete, it does show that dispersive terms alone are probably inadequate to explain the deviations of the evaporation rate from that predicted by the polydispersity alone. In addition, the incompleteness of the model does not alter the main thesis of the paper, which is that the polydisperse nature of the PFPE is the dominant factor accounting for the nonclassical evaporation kinetics of the thin film.

Acknowledgment. The authors thank Dan Castro for preparation of the thin film samples and his subsequent patient measurement of their thickness over time.

References and Notes

(1) Gellman, A. J. *Current Opin. Colloid Interface Sci.* **1998**, *3*, 368−372.
(2) Saperstein, D.; Lin, L. *Langmuir* **1990**, *6*, 1522.
(3) Vurens, G. H.; Gudeman, C. S.; Lin, L. J.; Foster, S. J. *IEEE Trans. Magn.* **1993**, *29*, 282.
(4) Kasai, P. H.; Tang, W. T.; Wheeler, P. *Appl. Surf. Sci.* **1991**, *51*, 201.
(5) Kasai, P. H.; Wheeler, P. *Appl. Surf. Sci.* **1991**, *52*, 91.
(6) Kasai, P. H. *Macromolecules* **1992**, *25*, 6791.
(7) Novotny, V. J. *J. Chem. Phys.* **1990**, *92*, 3189.
(8) O'Connor, T. M.; Jhon, M. S.; Bauer, C. L.; Min, B. G.; Yoon, D. Y.; Karis, T. E. *Tribol. Lett.* **1995**, *1*, 219.
(9) O'Connor, T. M.; Back, Y. R.; Jhon, M. S.; Min, B. G.; Yoon, D. Y.; Karis, T. E. *J. Appl. Phys.* **1996**, *79*, 5788.
(10) Min, B. G.; Choi, J. W.; Brown, H. R.; Yoon, D. Y.; O'Connor, T. M.; Jhon, M. S. *Tribol. Lett.* **1995**, *1*, 225.
(11) Ma, X.; Gui, J.; Smoliar, L.; Grannen, K.; Marchon, B.; Bauer, C. L.; Jhon, M. S. *Phys. Rev. E* **1999**, *59*, 722.
(12) Ma, X.; Gui, J.; Grannen, K.; Smoliar, L.; Marchon, B.; Jhon, M. S.; Bauer, C. L. *Phys. Rev. E* **1999**, *60*, 5795.
(13) Ma, X.; Bauer, C. L.; Jhon, M. S.; Gui, J.; Marchon, B. *Tribol. Lett.* **1999**, *6*, 9.
(14) Ma, X.; Gui, J.; Smoliar, L.; Grannen, K.; Marchon, B.; Jhon, M. S.; Bauer, C. L. *J. Chem. Phys.* **1999**, *110*, 3129.
(15) Mate, C. M.; Marchon, B. J. *Phys. Rev. Lett.* **2000**, *85*, 3902.
(16) Stirniman, M. J.; Falcone, S. J.; Marchon, B. J. *Tribol. Lett.* **1999**, *6*, 199.
(17) Stirniman, M. J.; Falcone, S. J. *Tribol. Lett.* **2000**, *8*, 171.
(18) Tyndall, G. W.; Waltman, R. J. *J. Phys. Chem. B* **2000**, *104*, 7085.
(19) Radhakrishnan, K.; Hindmarsh, A. C. *Description and Use of LSODE, the Livermore Solver for Ordinary Differential Equations*, NASA reference publication 1327, and Lawrence Livermore National Laboratory technical report UCRL ID-113855, March 1994.
(20) Paserba, K. R.; Gellman, A. J. *J. Phys. Chem. B* **2001**, *105*, 12105.
(21) Israelachvili, J. *Intermolecular and Surface Forces*; Academic Press: London, 1985.